A New Calibration Method of Line Scan Camera for High-Precision Two-Dimensional Measurement

Jiabin Zhang, Zhengtao Zhang, *Member, IEEE*, Fei Shen, Feng Zhang, Hu Su

***Abstract*—In this paper, a calibration method for line scan cameras with image distortion is proposed to perform high-precision planar measurement. The intrinsic parameter model is presented according to the imaging work principle of the line scan camera. Moreover, an improved camera model is proposed via integrating the perspective transformation with the extrinsic parameter model in the consideration of image distortion resulting from the non-parallelism of motion direction and object plane. On this basis, the parameters in above model are calibrated based on nonlinear damping least square method with a planar chessboard pattern. A set of measurement experiments are conducted and the results verify the effectiveness of proposed approaches.**

***Index Terms*—Line scan camera, camera calibration, distortion correction, visual measurement, planar measurement.**

I. Introduction

Line scan camera is widely applied to various fields such as industrial defect detection, precision measurement, biotechnology, traffic flow detection etc. Due to its capability of providing larger field of view with high resolution compared to conventional area array camera [1-7]. Tao et al. designed a novel instrument based on line scan imaging system to detect the surface flaw for a large aperture optical element with size of 810 mm×460 mm and achieved inspection precision is 3 μm [2]. An automated measurement system using line scan cameras is developed to detect edges and measure lengths of steel strips [4]. In addition to the industrial field, a line scan camera is successfully applied for a real penetration measurement system to ensure the pile can support the weight of structure in the process of building [5]. Line scan cameras are also utilized to measure the isolated cardiac muscle cell length [6], and tree ring length [7].

Line scan camera employs linear arrays to provide extended viewing areas by virtue of scanning motion. Thus, the work modes of line scan camera imaging system are generally classified into two categories: (i) the camera is moving while the object is stationary (CMOS); (ii) the object is moving while the camera is stationary (OMCS). The existing methods always utilize CMOS mode to acquire the full image due to the inconvenience of moving the object such as telemetry. On the contrary, OMCS mode is often adopted to fit for those applications where the objects are fast moving and high resolution is desired such as production line.

When it comes to use line scan camera for measurement, camera calibration is a necessary step to find the transformation relationship between the visual coordinate system and the measurement coordinate system. A two-step calibration method was proposed by Horaud to estimate the projection parameters of a 3-D point onto a straight line [8]. However, the results of calibration depend on the precision of the calibration pattern's displacements along Z-axis. Afterwards, improved calibration methods [9, 10] use a calibration pattern with 3-D façade whose coordinate of Z-axis is known in advance. Nevertheless, this type of approach needs a calibration pattern which is difficult to make. Besides, a two-stage calibration method for close-range photogrammetric applications is proposed by rigidly coupling the line scan camera to an auxiliary frame camera whose intrinsic parameters have been obtained in advance [11]. It is noted that using the auxiliary camera is an additional source of errors. A novel linear method is presented to estimate the intrinsic and extrinsic parameters of a 1D camera using a planar object instead of 3D landmarks. But the proposed model cannot be straightforwardly applied to solve world coordinates through image coordinates [12]. The above available calibration methods need either auxiliary devices or strict requirements which limited the application of these methods.

The motivation of this paper is to propose a calibration method for high precision 2-D measurement only using a planar chessboard. Different from the pin-hole model for the area array camera, the intrinsic parameter model of line scan camera is presented based on its imaging work principle. Moreover, an improved model integrating the perspective transformation is proposed to correct image distortion caused by the non-parallelism of motion direction and object plane. Then a three-stage approach based on nonlinear damping least square method is proposed to perform the calibration. The proposed calibration methods are verified on our designed imaging system.

The remaining of the paper is organized as follows. Section II introduces the line scan imaging system for the measurement. The line scan camera model is presented in Section III. The calibration method for the model is introduced in Section IV. Section V shows the experiment results and error analysis. Finally, the paper is concluded in Section VI.

II. Imaging System for High precision two-Dimensional Measurement

In this paper, an OMCS line scan camera imaging system is designed to perform 2-D planar measurement tasks with demand of high precision as shown in Fig. 1(a). The complete system includes a motion platform and a line scan camera visual system consist of a linear CCD and a spherical lens. The motion

This work is supported in part by the National Natural Science Foundation of China under Grant 61503378.

Authors are with the Research Center of Precision Sensing and Control, Institute of Automation, Chinese Academy of Sciences, Beijing 100190, China, also with University of Chinese Academy of Science, Beijing 100049, China. (e-mail: fei.shen@ia.ac.cn).

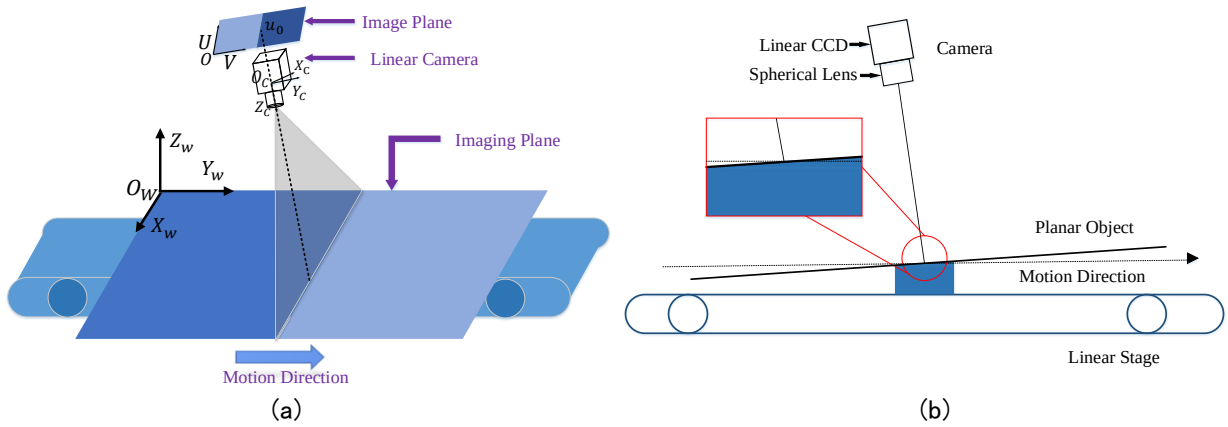

Fig. 1. The structure of line scan camera system and its coordinate systems.

platform is driven by a high-precision linear stage to help the camera acquire a full 2-D image.

To describe the camera model clearly, three categories of frames should be established first, including world coordinate system, camera coordinate system, and image coordinate system. As shown in Fig. 1(a), the world coordinate system labeled as $o_w x_w y_w z_w$ is set up on the imaging plane which coincides with $o_w x_w y_w$ and is perpendicular with $o_w z_w$. The camera coordinate system named as $o_c x_c y_c z_c$ whose $o_c z_c$ axis coincides with optic axis. ouv is image coordinate system whose axes ou and ov are parallel to $o_c x_c$ and $o_c y_c$ correspondingly.

To perform the planar measurement, it is essential to find the transform relationship between the image coordinate system and world coordinate system which is the main purpose of this paper. As shown in Fig. 1(b), the planar object is supported on the gripper which is mounted on the motion platform. In this case, the pose of planar object is decided on posture of gripper. Since the motion direction is inevitable non-parallel to the plane $o_w x_w y_w$ due to machining and installing error, the object distance varies with scanning motion in the process of imaging which leads to image distortion. The solution to correct this distortion is presented in the following section.

III. Line Scan Camera Model

A. Ideal Line Scan Camera Model

As described in the above section, the image distortion of the proposed line scan camera system is due to non-parallelism between the motion direction and the object plane. However, we first introduce ideal camera model which is in the condition that the motion direction is parallel to the plane $o_w x_w y_w$ without considering the distortion.

The complete ideal line scan camera model includes intrinsic parameter model and extrinsic parameter model. Concerning the intrinsic parameter model, the most widely used pin-hole model of area array camera is not suited to be used here. According to the imaging work principle of the line scan camera, the ideal intrinsic parameter model of line scan camera can be described as

$$\begin{bmatrix} z_c u \\ v \\ z_c \end{bmatrix} = \begin{bmatrix} k_x & 0 & u_0 \\ 0 & k_y & 0 \\ 0 & 0 & 1 \end{bmatrix} \begin{bmatrix} x_c \\ y_c \\ z_c \end{bmatrix} \tag{1}$$

where (u, v) and (x_c, y_c, z_c) are the coordinates of scene point in the image coordinate system and camera coordinate system respectively. k_x is the focal length of spherical lens and u_0 is the position of liner CCD's principal point in imaging array. Note that coordinate v only depends on the parameter k_y which represents the constant velocity of the motion platform driven by a high precision controller.

Then the extrinsic parameter model representing transform relationship between camera coordinate (x_c, y_c, z_c) and world coordinate (x_w, y_w, z_w) of scene point is expressed as

$$\begin{bmatrix} x_c \\ y_c \\ z_c \\ 1 \end{bmatrix} = \begin{bmatrix} \boldsymbol{R} & \boldsymbol{t} \\ 0 & 1 \end{bmatrix} \begin{bmatrix} x_w \\ y_w \\ z_w \\ 1 \end{bmatrix} = \begin{bmatrix} r_{11} & r_{12} & r_{13} & t_1 \\ r_{21} & r_{22} & r_{23} & t_2 \\ r_{31} & r_{32} & r_{33} & t_3 \\ 0 & 0 & 0 & 1 \end{bmatrix} \begin{bmatrix} x_w \\ y_w \\ z_w \\ 1 \end{bmatrix} \tag{2}$$

where $\boldsymbol{R}$ and $\boldsymbol{t}$ are the rotation matrix and translation vector respectively.

Furthermore, combining (1) and (2), the ideal line scan camera model with matrix form is written as

$$\begin{bmatrix} z_c u \\ v \\ z_c \end{bmatrix} = \begin{bmatrix} k_x & 0 & u_0 \\ 0 & k_y & 0 \\ 0 & 0 & 1 \end{bmatrix} \begin{bmatrix} r_{11} & r_{12} & r_{13} & t_1 \\ r_{21} & r_{22} & r_{23} & t_2 \\ r_{31} & r_{32} & r_{33} & t_3 \end{bmatrix} \begin{bmatrix} x_w \\ y_w \\ z_w \\ 1 \end{bmatrix} \tag{3}$$

Finally, as the coordinates z_w of scene points on the planar object equal zero, the ideal line scan camera model is obtained as

$$\begin{cases} m_{11} x_w + m_{12} y_w + m_{14} - m_{31} x_w u + m_{32} y_w u - u = 0 \\ m_{21} x_w + m_{22} y_w + m_{24} - v = 0 \end{cases} \tag{4}$$

where parameter vector $\boldsymbol{m}$ is written as

$$\boldsymbol{m} = \begin{bmatrix} m_{11} \\ m_{12} \\ m_{14} \\ m_{21} \\ m_{22} \\ m_{24} \\ m_{31} \\ m_{32} \end{bmatrix} = \begin{bmatrix} (k_x r_{11} + u_0 r_{31})/t_3 \\ (k_x r_{12} + u_0 r_{32})/t_3 \\ k_x t_1/t_3 + u_0 \\ k_y r_{21} \\ k_y r_{22} \\ k_y t_2 \\ r_{31}/t_3 \\ r_{32}/t_3 \end{bmatrix} \tag{5}$$

B. Improved Line Scan Camera Model with Distortion Correction

Considering the image distortion due to the non-parallelism of motion direction and object plane, a perspective transformation can represent the relationship between the real image coordinate (u_r, v_r) and ideal image coordinate (u, v) of scene points. To correct distortion, the transformation from real image point (u_r, v_r) to ideal image coordinate (u, v) is expressed as

$$\begin{bmatrix} u \\ v \end{bmatrix} = \begin{bmatrix} u_r/(au_r + bv_r + 1) \\ v_r/(au_r + bv_r + 1) \end{bmatrix} \tag{6}$$

Through adding the distortion correction to ideal camera model as given in (4), the line scan camera model with distortion correction is written as

$$\begin{cases} (au_r + bv_r + 1)[m_{11}x_w + m_{12}y_w + m_{14}] - m_{31}x_w u_r \\ \quad +m_{32}y_w u_r - u_r = 0 \\ (au_r + bv_r + 1)[m_{21}x_w + m_{22}y_w + m_{24}] - v_r = 0 \end{cases} \tag{7}$$

Essentially, calibration of a line scan camera aims to solve the model parameters for transforming image coordinate of scene points to their world coordinate. As shown in Fig. 1(a), the world coordinate system is set up on the imaging plane decided by the thickness of the planar calibration chessboard. It is noted that thickness of the planar object is always varied from the chessboard in practical application. Nevertheless, the plane $o_w x_w y_w$ of chessboard's world coordinate system is parallel to that of planar object. Therefore, in order to transform image coordinates of scene points on parallel object planes to their world coordinates through one calibration process, the extrinsic parameter t_3 in (3) is extracted out from parameter vector. The improved model with extracting the key parameter is expressed as

$$\begin{cases} (au_r + bv_r + 1)[m'_{11}x_w/t_3 + m'_{12}y_w/t_3 + m'_{14}/t_3 + u_0] \\ \quad -m'_{31}x_w u_r/t_3 + m'_{32}y_w u_r/t_3 - u_r = 0 \\ (au_r + bv_r + 1)[m'_{21}x_w + m'_{22}y_w + m'_{24}] - v_r = 0 \end{cases} \tag{8}$$

where the final parameter vector $\boldsymbol{x}$ of line scan camera model can be rewritten as

$$\boldsymbol{x} = \begin{bmatrix} m'_{11} \\ m'_{12} \\ m'_{14} \\ m'_{21} \\ m'_{22} \\ m'_{24} \\ m'_{31} \\ m'_{32} \\ a \\ b \\ t_3 \\ u_0 \end{bmatrix} = \begin{bmatrix} k_x r_{11} + u_0 r_{31} \\ k_x r_{12} + u_0 r_{32} \\ k_x t_1 \\ k_y r_{21} \\ k_y r_{22} \\ k_y t_2 \\ r_{31} \\ r_{32} \\ a \\ b \\ t_3 \\ u_0 \end{bmatrix} \tag{9}$$

It is emphasized that parameter t_3 characterizes the translation relationship between the plane $o_w x_w y_w$ of chessboard's world coordinate system and planar object's plane. Thus, for high precision parallel planar objects measurement tasks, only the parameter t_3 need to be modified manually instead of recalibration when the thickness of the measured object is changed.

IV. Model Calibration

A. Calibration for Ideal Model

For the ideal camera model in section III(A), least square method can be used to calibrate its parameter vector $\boldsymbol{m}$ with image coordinates and world coordinates of n scene points. The equation (4) can be written as

$$\boldsymbol{A}\boldsymbol{m} = \boldsymbol{B} \tag{10}$$

where

$$\boldsymbol{A} = \begin{bmatrix} x_{w1} & y_{w1} & 1 & 0 & 0 & 0 & -x_{w1}u & -y_{w1}u \\ 0 & 0 & 0 & x_{w1} & y_{w1} & 1 & 0 & 0 \\ \multicolumn{8}{c}{\cdots} \\ x_{wn} & x_{wn} & 1 & 0 & 0 & 0 & -x_{wn}u & -y_{wn}u \\ 0 & 0 & 0 & x_{wn} & x_{wn} & 1 & 0 & 0 \end{bmatrix} \tag{11}$$

$$\boldsymbol{B} = [u_1 \quad v_1 \quad \ldots \quad u_n \quad v_n]^T \tag{12}$$

Then, the parameter vector $\boldsymbol{m}$ is given as

$$\boldsymbol{m} = (\boldsymbol{A}^T\boldsymbol{A})^{-1}\boldsymbol{A}^T\boldsymbol{B} \tag{13}$$

B. Calibration for Improved Model Based on Nonlinear Damping Least Squares Method

Now, using (8) and n sets image coordinates and world coordinates of n scene points, we can form $2n$ equations with unknown parameter vector $\boldsymbol{x}$. The nonlinear overdetermined equations are expressed as

$$\begin{cases} f_{11}(\boldsymbol{x}) = 0 \\ f_{21}(\boldsymbol{x}) = 0 \\ \cdots \\ f_{1n}(\boldsymbol{x}) = 0 \\ f_{2n}(\boldsymbol{x}) = 0 \end{cases} \tag{14}$$

where $f_{1i}(\boldsymbol{x}) = (au_{ri} + bv_{ri} + 1)[m'_{11}x_{wi}/t_3 + m'_{12}y_{wi}/t_3 + m'_{14}/t_3 + u_0] - m'_{31}x_{wi}u_{ri}/t_3 + m'_{32}y_{wi}u_{ri}/t_3 - u_{ri}$, and $f_{2i}(\boldsymbol{x}) = (au_{ri} + bv_{ri} + 1)[m'_{21}x_{wi} + m'_{22}y_{wi} + m'_{24}] - v_{ri}$. To solve these overdetermined equations precisely, they can be translated into a form of quadratic functional $\Theta(\boldsymbol{x})$ as

$$\Theta(\boldsymbol{x}) = \frac{1}{2}f(\boldsymbol{x})^T f(\boldsymbol{x}) = \frac{1}{2}\sum_{i=1}^{2m} f_i^2(\boldsymbol{x}) \tag{15}$$

Hence, the minimum value of function $\Theta(\boldsymbol{x})$ denoted as $\boldsymbol{x}^*$ is the least-squares solution of the over-determined equations $f(\boldsymbol{x}) = 0$ and expressed as

$$\Theta(\boldsymbol{x}^*) = \min_{x \in R^n} \Theta(\boldsymbol{x}) = \min_{x \in R^n} \frac{1}{2}f(\boldsymbol{x})^T f(\boldsymbol{x}) \tag{16}$$

Therefore, the solvent of the over-determined equations can be achieved by searching the minimum value of multi-function $\Theta(\boldsymbol{x})$. If $f(\boldsymbol{x})$ is differential in the domain, the gradient of $\Theta(\boldsymbol{x})$ denoted as $g(\boldsymbol{x})$ is set to be zero as follows:

$$g(\boldsymbol{x}) =\because \Theta(\boldsymbol{x}) = \frac{1}{2}Df(\boldsymbol{x})^T f(\boldsymbol{x}) = 0 \tag{17}$$

where

$$Df(\boldsymbol{x})^T = \begin{bmatrix} \frac{\partial f_{11}}{\partial m'_{11}} & \frac{\partial f_{12}}{\partial m'_{11}} & \cdots & \frac{\partial f_{2n}}{\partial m'_{11}} \\ \frac{\partial f_{11}}{\partial m'_{12}} & \frac{\partial f_{12}}{\partial m'_{12}} & \cdots & \frac{\partial f_{2n}}{\partial m'_{12}} \\ \vdots & \vdots & \vdots & \vdots \\ \frac{\partial f_{11}}{\partial u_0} & \frac{\partial f_{12}}{\partial u_0} & \cdots & \frac{\partial f_{2m}}{\partial u_0} \end{bmatrix}$$

The Taylor's expansion of $f(\boldsymbol{x})$ at the point $\boldsymbol{x}^{\mathrm{k}}$ can be expressed as

$$f(\boldsymbol{x}) \approx f(\boldsymbol{x}^{\mathrm{k}}) + Df(\boldsymbol{x}^{\mathrm{k}})(\boldsymbol{x} - \boldsymbol{x}^{\mathrm{k}}) \tag{18}$$

With substituting the above equation into (17) and adding the damping item $\mu_k I$[13, 14], the iterative $\boldsymbol{x}^{k+1}$ can be obtained as

$$\boldsymbol{x}^{k+1} = \boldsymbol{x}^{k} - G'(\boldsymbol{x}^{k})^{-1} Df(\boldsymbol{x}^{k})^{T} f(\boldsymbol{x}^{k}) \quad (20)$$

where $G'(\boldsymbol{x}^{k}) = Df(\boldsymbol{x}^{k})^{T} Df(\boldsymbol{x}^{k}) + \mu_k I$.

Based on the above principles, specific steps for calibrating linear camera model system are as follows:

1) Sample n sets of scene points with their world coordinate (x_w, y_w) and image coordinate (u_r, v_r) on an image of planar chessboard, and then form $2n$ equations according to equation (14).

2) Calculate the iterative matrix $G'(\boldsymbol{x}^{k})$.

3) Solve unknown parameter vector x by applying the iteration formula (20). Specifically, the iterative process starts with a selected initial value and stops until the 2-norm of the two adjacent vectors' error becoming smaller than threshold value.

V. Experiments

To verify the calibration method we proposed, a series of experiments were implemented on the hardware platform as shown in Fig. 2, whose structure has been illustrated in Fig. 1. The pixel size, sensor size and the depth of field of the line scan camera in the platform are 12 μm×12 μm, 8192 *pixels* × 1 *line* and 1 *mm* respectively. In addition, the motion platform is driven by a high-precision linear stage to help the camera acquire a full 2-D image.

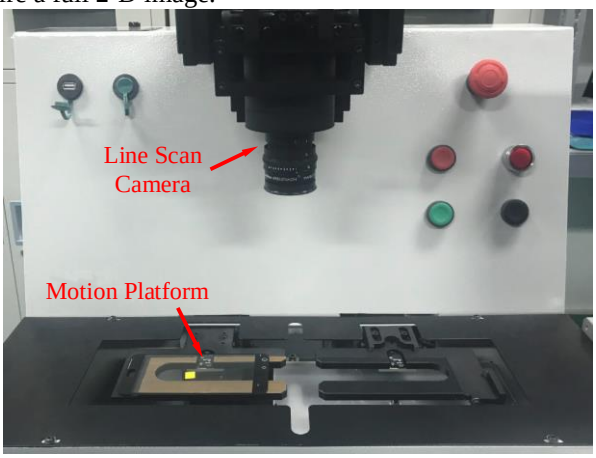

Fig. 2. Structure of hardware platform of our imaging system.

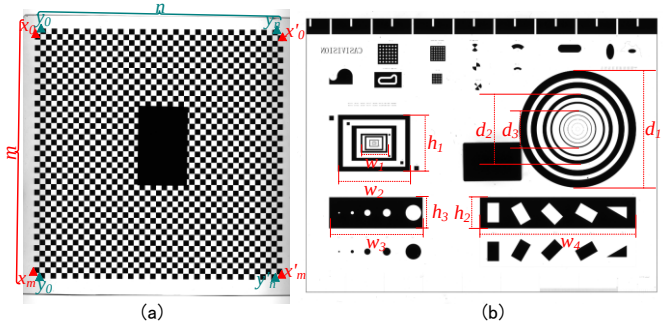

Fig. 3. The image of chessboard and standard board: (a) the image of calibration chessboard, the dark rectangle in the center is a sucker to fix the chessboard on the linear motion stage; (b) the image of standard board.

TABLE I
Specifications of Chessboards

No.	Thickness	Number of Checks and Size
1	0.5mm	45×45 checks of 2×2mm
2	0.7mm	45×45 checks of 2×2mm
3	1.0mm	45×45 checks of 2×2mm

The planar chessboards with different thickness and a standard board are employed to perform the calibration and validation experiments. The specifications of the planar chessboards are given in the Table I and the images of chessboard and standard board are shown in Fig. 3. Specifically, based on the calibration steps presented in the above section, an image of no.1 chessboard is utilized to perform the calibration. By sampling the world coordinates and image coordinates of all the corner points, the parameter vector $\boldsymbol{x}^*$ in (9) is obtained as

$\boldsymbol{x}^*$ = [84.817, 0.357, 268.181, 0.480, 84.746, 4192.104, 6.0828, 8.593e-005, 8.593e-007, 3.0917e-009, -3.152e-008, 268.181, 0.996]^T

Furthermore, other planar chessboards with different thickness and standard board are utilized to do the further validation. Three groups of experiments are conducted in the following. Firstly, a contrast experiment for the distortion correction is performed on several images of no.1 chessboard. Secondly, the images of no.2 and no.3 chessboard are utilized to verify that our calibration method is suitable for multi-parallel-planar measurement. Thirdly, the images of standard board are utilized to further verify the accuracy of our calibration method.

A. Contrast Experiment for the Two Models

Eight images are acquired to perform the experiment by placing the no.1 chessboard in eight random angles that from -5 degrees to 5 degrees on plane $o_w x_w y_w$. Using the above model parameter vector x^*, we can calculate the world coordinates of the corner points in the images through the camera model with distortion correction (8). Correspondingly, the corner points' world coordinates can also be obtained through the camera model without distortion correction (4) by using the model parameter vector $\boldsymbol{m}$ in (5). The two measurement errors e_{x_i} and e_{y_i} are designed to verify the calibration method. Specifically, $e_{x_i} = \Delta x_i - \Delta x_i{}^*$, where Δx_i is the Euclidean distance of x_i and x'_i marked in Fig. 3(a). x_i and x'_i are the leftmost and rightmost corner points of the chessboard's each row. $\Delta x_i{}^*$ is the standard value of Δx_i and i is the number of m rows. Similarly, $e_{y_j} = \Delta y_j - \Delta y_j{}^*$, where y_j and y'_j are the top and bottom corner points of the chessboard's each column, j is the number of n columns.

As shown in Fig. 4(a) and (b), using the model without distortion correction, the measurement errors e_{x_i} and e_{y_j} are in the range of [-0.030, 0.005] *mm* and [-0.025, 0.0] *mm* respectively. Contrastively, the model with distortion correction is proved to have good performance of controlling the measurement errors e_{x_i} and e_{y_j} in the range of [-0.006, 0.012] *mm* and [-0.005, 0.0] *mm* respectively.

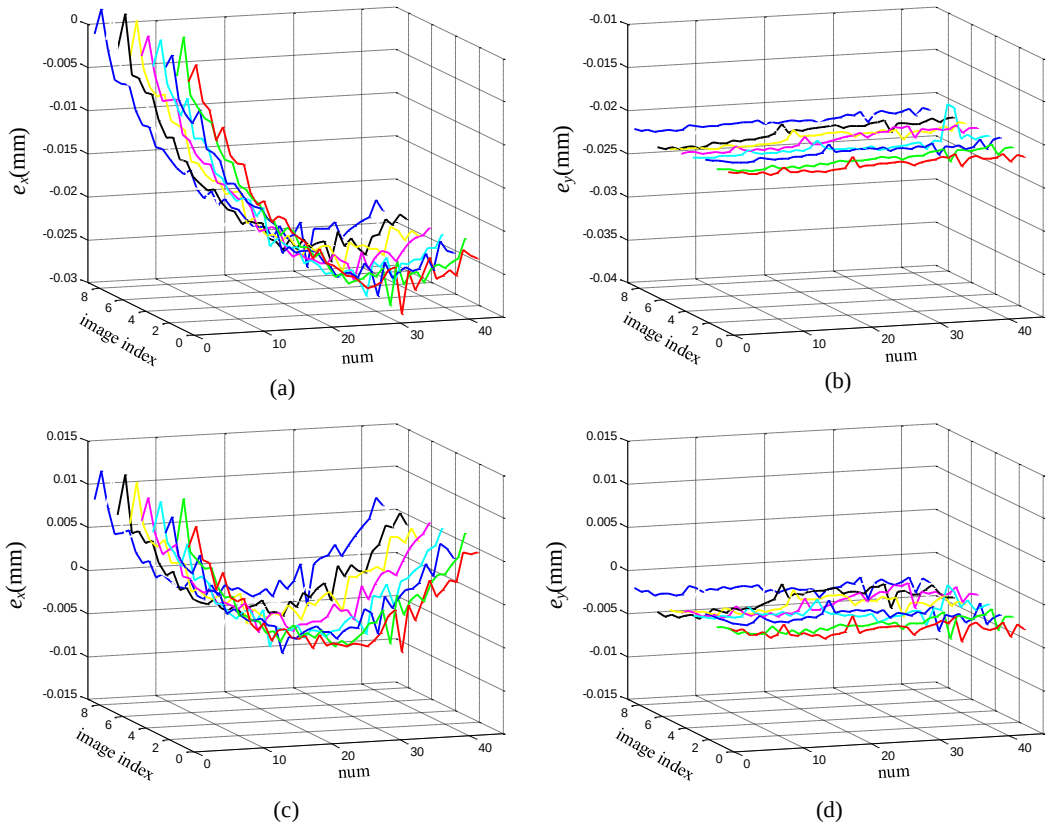

Fig. 4. Results of contrast experiment for the distortion correction: (a) errors of Δx_i without distortion correction; (b) errors of Δy_j without distortion correction; (c) errors of Δx_i with distortion correction; (d) errors of Δy_j with distortion correction.

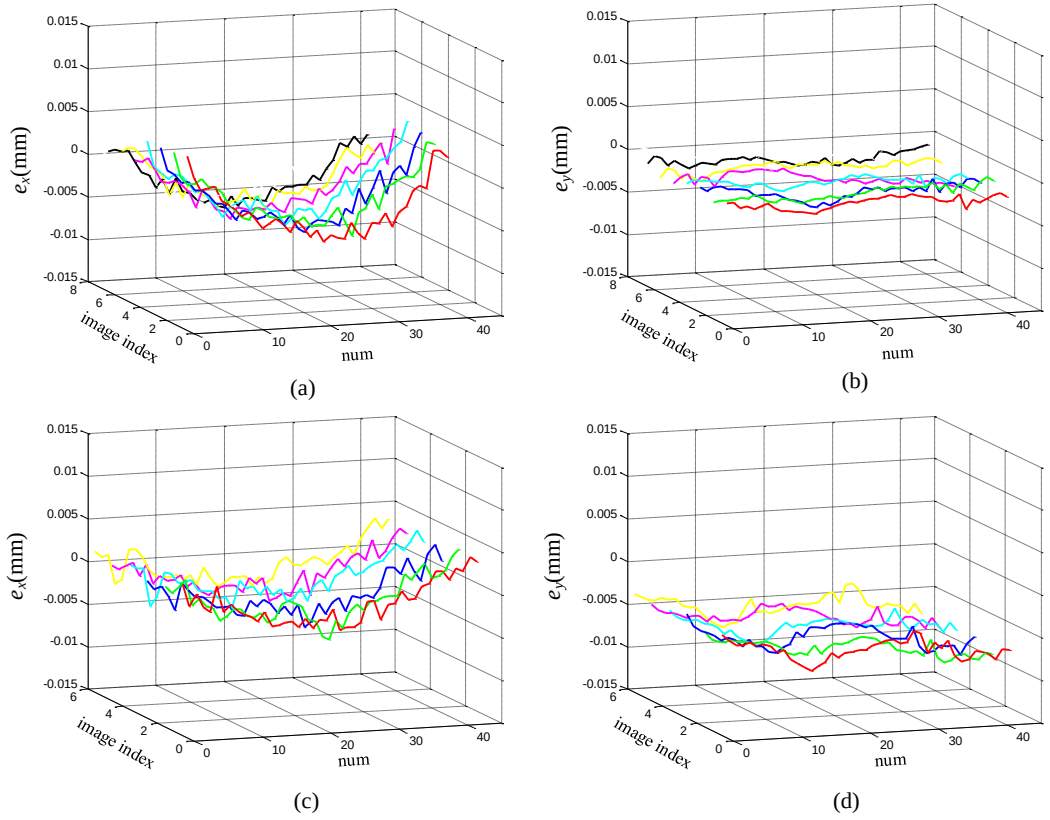

Fig. 5. Result of verification of the calibration method on parallel-planes: (a) errors of Δx_i on no.2 chessboard; (b) errors of Δy_j on no.2 chessboard; (c) errors of Δx_i on no.3 chessboard; (d) errors of Δy_j on no.3 chessboard.

B. *Model Verification on Parallel Planes*

The above experiment results reveal that the line scan camera model could have good performance in the measurement task on the one fixed 2-D plane calibrated. Moreover, as the parameter t_3 can be extracted from our model depicted in (8), the relative measurement error caused by different thickness of planar objects can also be eliminated. Similar to the above experiment, eight images of no.2 chessboard and six images of no.3 chessboard are acquired respectively to perform the experiment by placing the chessboards in different random angles. As shown in Fig. 5, the absolute errors of all Δx_i and Δy_j are less than 0.010 *mm*.

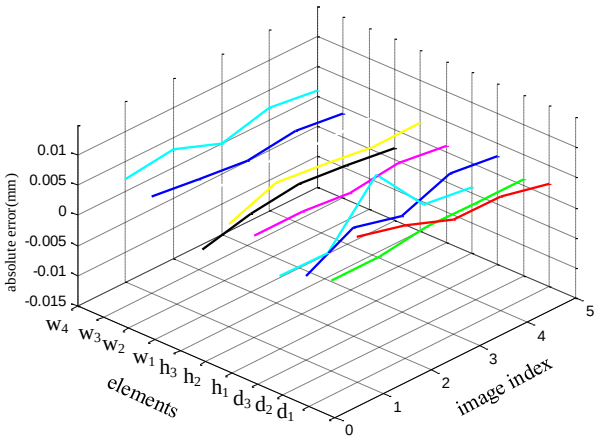

Fig. 6. Result of verification of the calibration method using standard board

TABLE II
MEASUREMENT RESULTS OF STANDARD BOARDS

Elements	Standard value	measurement errors
d_1	30mm	0.002mm ~ 0.009mm
d_2	18mm	0 ~ 0.001mm
d_3	9.5mm	-0.001mm ~ 0.004mm
h_1	14.5mm	-0.004mm ~ 0.006mm
h_2	8mm	0.001mm ~ 0.002mm
h_3	8mm	0.002mm ~ 0.005mm
w_1	9mm	-0.004mm ~ -0.001mm
w_2	18.5mm	0 ~ 0.002mm
w_3	24mm	-0.001mm ~ 0.001mm
w_4	40mm	0 ~ 0.003mm

C. *Test on Standard Board*

To ensure our calibration method be suitable for the applications for high-precision measurement, verification experiment of calibration method is performed on standard board. Five images are acquired to perform the experiment by placing the standard board in five random angles that from -5 degrees to 5 degrees on plane $o_w x_w y_w$. Sizes of all the ten elements marked in the image of standard board shown in Fig. 3(b) are calculated by using the line scan camera model and model parameter vector that obtained by the image of no.1 chessboards. Table II and Fig. 6 shows the standard value of the elements' sizes and the measurement errors. In all cases, as the pixel size of the line scan camera is 12 μm×12 μm, the absolute errors that are less than 0.010 *mm* that can meet the requirement of most industry high-precision measurement tasks.

VI. CONCLUSION

A line scan camera calibration method with distortion correction for high-precision planar measurement is developed in this paper. The intrinsic parameter model for line scan cameras is presented. Furthermore, an improved measurement model combining with perspective transformation is proposed to correct image distortion caused by the non-parallelism of motion direction and object plane. A three-stage calibration method only using a planar chessboard is presented. The obtained parameters are used to solve world coordinates from image coordinates. Experiments demonstrate the effectiveness of the proposed method. The planar measurement accuracy is 10 μm.

REFERENCES

[1] K. Hirahara and K. Ikeuchi, "Detection of street-parking vehicles using line scan camera and scanning laser range sensor," in Intelligent Vehicles Symposium, 2003. Proceedings. IEEE, 2003, pp. 656-661: IEEE.

[2] X. Tao, Z. Zhang, F. Zhang, and D. Xu, "A novel and effective surface flaw inspection instrument for large-aperture optical elements," IEEE Transactions on Instrumentation and Measurement, vol. 64, no. 9, pp. 2530-2540, 2015.

[3] C. A. Luna et al., "Method to measure the rotation angles in vibrating systems," IEEE transactions on instrumentation and measurement, vol. 55, no. 1, pp. 232-239, 2006.

[4] Y.-S. Li, T. Y. Young, and J. A. Magerl, "Subpixel edge detection and estimation with a microprocessor-controlled line scan camera," IEEE Transactions on Industrial Electronics, vol. 35, no. 1, pp. 105-112, 1988.

[5] M.-S. Lim and J. Lim, "Visual measurement of pile movements for the foundation work using a high-speed line-scan camera," Pattern Recognition, vol. 41, no. 6, pp. 2025-2033, 2008.

[6] P. J. Harris, D. Stewart, M. C. Cullinan, L. M. Delbridge, L. Dally, and P. Grinwald, "Rapid measurement of isolated cardiac muscle cell length using a line-scan camera," IEEE Transactions on Biomedical Engineering, no. 6, pp. 463-467, 1987.

[7] R. Guay, R. Gagnon, and H. Morin, "A new automatic and interactive tree ring measurement system based on a line scan camera," The Forestry Chronicle, vol. 68, no. 1, pp. 138-141, 1992.

[8] R. Horaud, R. Mohr, and B. Lorecki, "On single-scanline camera calibration," IEEE Transactions on Robotics and Automation, vol. 9, no. 1, pp. 71-75, 1993.

[9] C. A. Luna, M. Mazo, J. L. Lázaro, and J. F. Vazquez, "Calibration of line-scan cameras," IEEE Transactions on Instrumentation and Measurement, vol. 59, no. 8, pp. 2185-2190, 2010.

[10] E. Lilienblum, A. Al-Hamadi, and B. Michaelis, "A coded 3D calibration method for line-scan cameras," in German Conference on Pattern Recognition, 2013, pp. 81-90: Springer.

[11] B. Hui, G. Wen, P. Zhang, and D. Li, "A novel line scan camera calibration technique with an auxiliary frame camera," IEEE Transactions on Instrumentation and Measurement, vol. 62, no. 9, pp. 2567-2575, 2013.

[12] J. Draréni, S. Roy, and P. Sturm, "Plane-based calibration for linear cameras," International Journal of Computer Vision, vol. 91, no. 2, pp. 146-156, 2011.

[13] J. J. Moré, "The Levenberg-Marquardt algorithm: implementation and theory," in Numerical analysis: Springer, 1978, pp. 105-116.

[14] F. Shen, W. Wu, D. Yu, D. Xu, and Z. Cao, "High-precision automated 3-D assembly with attitude adjustment performed by LMTI and vision-based control," IEEE/ASME Transactions on Mechatronics, vol. 20, no. 4, pp. 1777-1789, 2015